RASĀYAN *J. Chem.*
Vol. 19 | No. 1 | 207-216 | January-March | 2026
ISSN: 0974-1496 | e-ISSN: 0976-0083 | CODEN: RJCABP
http://www.rasayanjournal.com
http://www.rasayanjournal.co.in

IMPROVING LIQUID SMOKE YIELD FROM COCONUT SHELLS VIA MICROWAVE-ASSISTED PYROLYSIS WITH SELECTED CARBON ABSORBENTS

S.P.A. Anggraini[1,✉], A.C.K. Fitri[1], F.K. Widyastuti[1], M. Mahfud[2], M.F. Rizki[3], B. Prihatiningsih[4], T. Sari[5], B. Sardi[6], N. Indayaningsih[6], A. Hapid[7], N.I.F. Nisa[8], A. Aminudin[9], and J. Surif[10]

[1]Department of Chemical Engineering, Tribhuwana Tunggadewi University, Malang-65144, Indonesia
[2]Department of Chemical Engineering, Sepuluh Nopember Institute of Technology, Surabaya-60111, Indonesia
[3]Department of Chemistry, Tadulako University, Palu-94118, Indonesia
[4]Department of Civil Engineering, Merdeka University, Malang-65146, Indonesia
[5]Department of Civil Engineering, Universitas 17 Agustus 1945, Surabaya-60111, Indonesia
[6]Research Centre for Energy Materials, National Research and Innovation Agency (BRIN), South Tangerang-15314, Indonesia
[7]Research Centre for Mining Technology, National Research and Innovation Agency (BRIN), South Tangerang-15314, Indonesia
[8]Department of Chemical Engineering, Universitas PGRI Madiun, Madiun-63117, Indonesia
[9]Automotive Engineering Technology, Politeknik Negeri Madiun, Madiun-63133, Indonesia
[10]Department of Education Science, Mathematics & Multimedia Creative, School of Education, Faculty of Social Science & Humanities, Universiti Teknologi Malaysia, Johor Bahru-81310, Johor, Malaysia
✉Corresponding author: abrina@unitri.ac.id

ABSTRACT

The growing concern about the safety of synthetic preservatives has led to a greater demand for natural options, such as liquid smoke. This research investigates the generation of liquid smoke from coconut shells through microwave-assisted pyrolysis. The focus is specifically on the effects of different carbon absorbents under various operating conditions on the process. Activated charcoal, biochar, and regular charcoal were used. Temperatures of 180, 230, and 280°C, particle sizes of 1, 2, and 3 mm, and heating durations of 5, 10, 15, 20, 25, and 30 minutes were all predetermined. The results of this study found that activated charcoal was the most effective absorber, reaching 114.67% efficiency at 3 mm. The yield of liquid fumes was greatly influenced by temperature and particle size. At 180℃, 2 mm particles gave the highest yield (23.99%), while at 230 and 280℃, 3 mm particles gave better results (30.43% and 34.40%). Overall, the best yield was 31.13% achieved at 255℃, particle size of 2.8 mm, and 28.7 min heating. These results show that choosing the right carbon absorbent and setting the operating conditions really matter for making good liquid smoke with microwave-assisted pyrolysis.

Keywords: Activated Charcoal; Carbon Absorbent; Coconut Shell; Liquid Smoke; Microwave-Assisted Pyrolysis.

INTRODUCTION

The use of formalin as a food preservative in Indonesia remains a significant concern. The data show that 66% of the 786 fish samples tested contain formalin.[1] This compound is harmful to health because it can bind to the proteins of the human body, with a safe threshold of only 0.2 mg/kg of body weight.[2] This condition encourages the need for safer natural preservative alternatives, one of which is liquid smoke.

Liquid smoke is produced through the pyrolysis process of biomass such as coconut shells, wood, or rice husks. The pyrolysis process produces active compounds such as phenols, carbonyls, and organic acids that function as antimicrobials and antioxidants,[3–6] so that it has a longer shelf life. One of the raw materials for making liquid smoke, coconut shell, is an ideal raw material because of its high lignin content (29.4%), which produces optimal phenolic compounds in liquid smoke, so it can be used as a food preservative that acts as an antioxidant and antimicrobial.[7] Liquid smoke from coconut shells showed peak yields of phenols (7.32%) at 600°C for 120 min, acetic acid (92.30%) at 500°C for 120 min, and carbonyls (32.56%) at 400°C for 60 min.[6,8,9] According to Hasan Ashari Oramahi *et al.* (2022) claimed that at 440°C, the production of liquid smoke from coconut shells was 31.31% and the pyrolysis process time was 124 min.[10] The development of liquid smoke in Indonesia is certainly very promising, because the basic material for making its biomass waste is quite abundant in Indonesia. The potential for the utilisation of coconut shell waste is very abundant.[11] One promising technique for producing liquid smoke is Microwave-Assisted Pyrolysis (MAP). Compared to conventional pyrolysis, this method provides more uniform heating, shorter reaction times, and greater energy efficiency.[12,13] The process is further enhanced with the use of microwave absorbers, such as activated carbon, which efficiently capture the energy of the microwave then convert the energy into heat.[14–18]

EXPERIMENTAL

Materials and Equipment

The raw material in this study was coconut shells obtained from the Dampit area of Malang. The water used as a coolant in the condenser was well water. Different types of carbon absorbents are activated charcoal, biochar, and regular charcoal. Instruments included TGA, GC-MS and microwave-assisted pyrolysis.

Experiment Apparatus

The main equipment used was an 800W, 220V microwave with a 1250W input, operating at 2450 MHz and measuring 48.5 × 37 × 29.25 cm. This MAP method used a two-brand Pyrex neck flask with a size of 500 mL (d = 9.85 cm). The pyrolysis setup included a condenser and a cooling trap for collecting tar-heavy fractions and light fractions of liquid smoke. In addition, it was also equipped with a temperature control on the microwave to control the desired temperature.

Procedure Experiment

Coconut shells were first dried in sunlight and then ground into particle sizes of 1, 2, and 3 mm. For each experiment, 50 grams of the dried shell particles were combined with a microwave absorber-activated charcoal, biochar, or regular charcoal at a proportion of 10% of the weight of the entire combination. Heating is applied to the mixture of ingredients using MAP at 180–280°C for 5–30 minutes. The pyrolysis process produced three fractions: light gas, heavy tar, and solid charcoal. The light gas passed through the condenser, where it cooled and condensed into liquid fumes. The non-condensed methane gas was released, and the viscous liquid smoke was captured in the cooling trap. After the solid charcoal was pyrolysed, the heavy tar was collected and stored separately after passing through the condenser. 50 g of coconut shells and two flask necks were placed in a microwave along with a 10% reducer. Different heat levels and periods during pyrolysis resulted in smoke, which was then condensed. Condensers were used for condensation and cooling, which produced liquid fumes. In the cooling trap, viscous liquid smoke was collected. Any remaining smoke that was not collected in the cooling trap and passed to a second condenser produced tar. During this procedure, the resulting tar was collected and stored in different storage places. The percentage of liquid smoke yield was one of the important components in assessing the quality of the process. The yield was computed as a proportion of the raw materials utilised; greater results indicated better quality processes. The following Eq.-1 was used to calculate the percentage of liquid smoke yield[19]:

$$Yield\ (\%) = \frac{weight\ of\ liquid\ smoke\ (gr)}{weight\ of\ raw\ material\ (gr)}\ x\ 100\% \qquad (1)$$

Analysis of Chemical Components of Liquid Smoke

The liquid smoke's chemical composition was determined through Gas Chromatography–Mass Spectrometry (GC–MS) analysis. First, the raw liquid smoke was extracted with ether, and the ether fraction containing the target compounds was separated and collected. This step was repeated several times, and the collected ether fraction was then combined and concentrated with the help of a nitrogen gas stream until about 1 mL remained. The GC-MS apparatus was then used to analyse the concentrated sample under particular parameters, such as EI ionisation at 70 eV, injector and detector temperatures of 290°C and 280°C, and a 30-meter Rtx-5MS column. The column temperature rose from 70°C to 230°C at 5°C/min, using helium as the carrier gas (60 mL/min, 13.7 kPa).

Response Surface Approach for Optimisation

The pyrolysis process for liquid smoke production was optimised using Response Surface Methodology (RSM). The three main operational variables analysed were the raw material's size (1, 2, and 3 mm), heating time (5-30 min), and microwave temperature (180, 230, and 280°). The study used Design Expert Program version 13 software with an FCCD design, which resulted in 20 experimental units to identify optimal conditions. Thus, the RSM served to determine the best combination of these three important factors (temperature, size, and time) to increase the amount of liquid smoke that can be produced from coconut shells, as indicated in Table-1.

Table-1: Range and Level of Independent Variables

Variables	Symbol coded	Range and levels		
		-1	0	1
Temperature (°C)	X_1	180	230	280
Size (mm)	X_2	1	2	3
Time (minute)	X_3	10	20	30

Regression analysis was applied to estimate the response function, leading to the development of first-order polynomial equations, as presented in Eq.-2:

$$Y = \beta_0 + \sum_{i=1}^{k} \beta_i X_i + \sum_{i=1}^{k} \beta_{ii} X_i^2 + \sum_{i-1}^{k-1} \sum_{j=2}^{k} \beta_{ij} X_i X_j + \varepsilon \quad (2)$$

The expected response (Y) was predicted using first-order polynomial regression equations. In this equation, there was a regression constant, whereas $\beta_0 \beta_i$, $\beta_{ii} \beta_{ij}$ was a coefficient representing the linear, square, and interaction effects of variables coded (x_i,) and $x_j \varepsilon$ The error model was denoted by ε.[10]

RESULTS AND DISCUSSION

TGA (Thermogravimetric Analysis) of Coconut Shell

Figure-1 presents the TGA/DSC curve of an 8.0239 mg coconut shell sample analysed under inert conditions, heated from 0–600°C at 10°C/min. TGA was used to measure changes in sample weight as temperature or time increased.

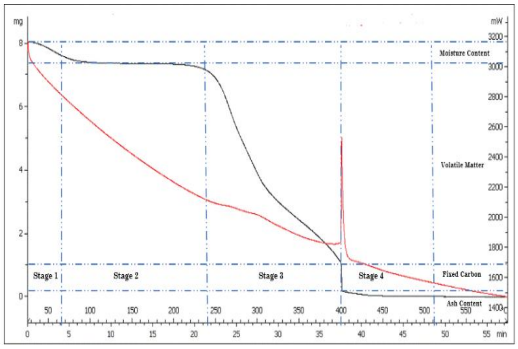

Fig.-1: Coconut Shell Analysis using TGA and DSC. TGA/DSC Curve (TGA is black and DSC is red)

Analysis of the TGA and DSC shows that the thermal degradation of coconut shells takes place in four

main stages, as shown in Fig.-1. The first stage begins at a temperature of about 65–68°C, characterised by water evaporation and a decrease in mass of about 6%. The second stage (65–240°C) involves the decomposition of hemicellulose as well as the release of volatile compounds such as furfural and acetic acid with a mass decrease of ±9%. The third stage (240–400°C) is the main phase of cellulose and lignin decomposition, producing compounds such as phenol and carbonyl, with a mass reduction of up to 96%. At this point, the DSC curve indicates an exothermic peak around 400°C, releasing approximately 2520 MW of heat. The fourth stage (400–512°C) shows the further decomposition of lignin and other heavy compounds with an additional mass decrease of ±10%. Overall, these results show that the thermal stability of coconut shells is affected by the content of water, hemicellulose, cellulose, and lignin that decompose gradually as the temperature increases.

Comparison Yield of the Effectiveness of Different Carbon Absorbers

Table-2 displays the yield comparison of various carbon absorbers in terms of creating liquid smoke.

Table-2: Comparison of Effectiveness using Various Kinds of Carbon Absorbents

Temperature (℃)	Absorbent Type	Material Size	Effectiveness (%)
180	Activated charcoal	1 mm	57.10
		2 mm	79.97
		3 mm	69.70
230	Activated charcoal	1 mm	68.63
		2 mm	87.57
		3 mm	101.43
280	Activated charcoal	1 mm	78.17
		2 mm	90.87
		3 mm	114.67
180	Biochar	1 mm	43.37
		2 mm	66.96
		3 mm	54.90
230	Biochar	1 mm	49.30
		2 mm	74.33
		3 mm	103.29
280	Biochar	1 mm	67.27
		2 mm	83.60
		3 mm	103.71
180	Regular charcoal	1 mm	37.13
		2 mm	51.03
		3 mm	47.50
230	Regular charcoal	1 mm	46.42
		2 mm	62.93
		3 mm	82.34
280	Regular charcoal	1 mm	60.71
		2 mm	76.60
		3 mm	99.41

Table-2 shows that activated charcoal had the highest effectiveness (114.67%) at a particle size of 3 mm, followed by biochar and regular charcoal. This is because activated charcoal has the largest porosity and surface area, so it is able to absorb and transfer microwave energy efficiently.[20] The heat generated is evenly distributed, accelerating the decomposition of biomass and increasing the production of liquid fumes.[21] The effectiveness increases with the particle size to the optimal point, which is 3 mm. Particles that are too small (1 mm) easily overheat and cause the formation of non-condensable gases, while 3 mm provides the best balance of energy absorption and penetration. Temperature also plays an important role; an Increase from 180°C to 280°C increases the effectiveness of all types of absorbents.[22] The best conditions are achieved at 280°C with 3 mm of activated charcoal. Activated charcoal utilises high temperatures more efficiently due to its large surface area and micropores (500–1500 m^2/g)[23], accelerating

the thermal degradation of biomass and producing liquid smoke with optimal phenol and carbonyl content.[24] The porous structure and functional group of oxygen facilitate the conversion of microwave energy into even heat, making it the most effective absorbent in the microwave pyrolysis process.[25]

Comparison of Absorbent Type Use to Liquid Smoke Yield using a MAP

The total use of absorbents in coconut shell raw materials for the manufacture of liquid smoke produced differences in liquid smoke yields. The type of absober affected the yield of liquid smoke. This was displayed in Fig.-2 below.

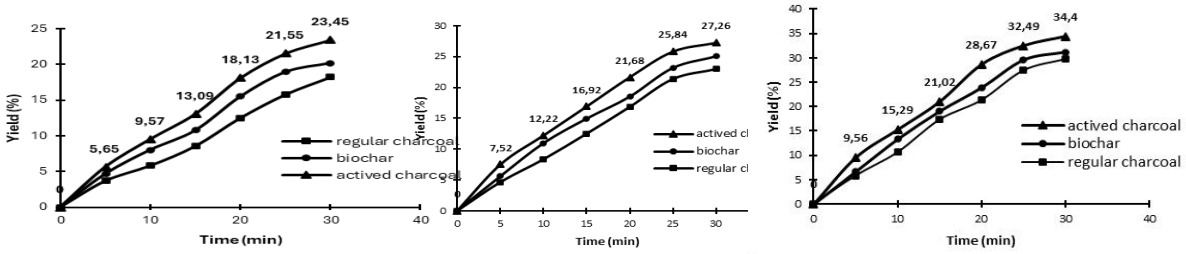

(a) (b) (c)

Fig.-2: Percentage Comparison of Results using different Types of Carbon Absorbent using the MAP Method (a) Particle Size 1 mm; (b) Particle Size 2 mm; (c) Particle Size 3 mm

Activated carbon is particularly effective as an absorber of electromagnetic waves due to its extensive and complex pore structure. The waves are not reflected, but enter and are trapped inside the pores until they lose energy, thus increasing the efficiency of radiation absorption.[26,27] Large surface area allows for more interaction with waves, while high thermal conductivity helps to efficiently absorb and disperse heat. Double reflection in the pores strengthens radiation absorption.[28] Increased conductivity is proportional to increased pore size.[29] Activated charcoal serves as a microwave absorber during the pyrolysis of coconut shells, speeding up heating and enhancing the quality of the liquid fumes. Without activated charcoal, liquid smoke remains formed, but with lower purity.[30] Microwaves accelerate pyrolysis reactions through the mechanism of dipole rotation and ionic conduction. The charged molecules move along the electric field of microwaves, causing an intermolecular collision and increasing the reaction activation energy.[31] Heating occurs evenly without direct contact, resulting in efficient heat distribution and shorter processing times.[32]

Comparison of Material Size to Liquid Smoke Yield using MAP

Using different coconut shell sizes affected liquid smoke yield, as shown in Fig.-3. Figures-3(a), 3(b), and 3(c) show yield variations at 180°C, 230°C, and 280°C for different material sizes. At 180℃, the highest yield was 2 mm particle size of 23.99%. Meanwhile, at 230 and 280°C, the highest yield was produced at 3 mm sizes of 30.43% and 34.40%. This was explained by the principle of mass displacement. One key factor affecting liquid smoke yield was coconut shell particle size.

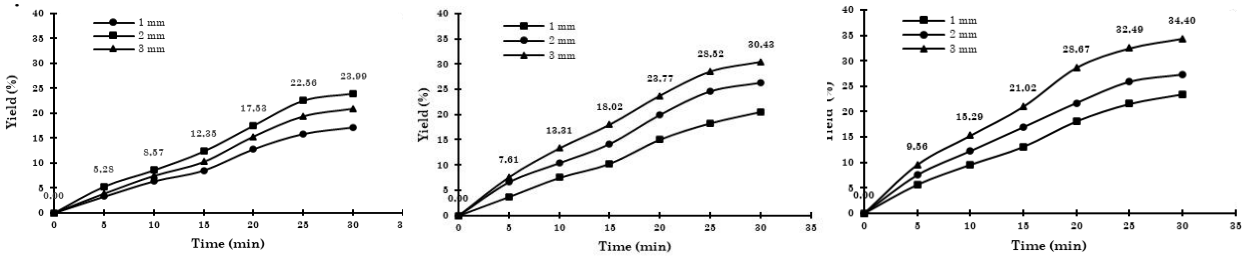

(a) (b) (c)

Fig-3: Percentage Comparison of Results using different Particle Sizes using the MAP Method: (a) 180 °C; (b) 230 °C; (c) 280 °C

During the pyrolysis of coconut shell, particle size significantly influences the evaporation kinetics and product distribution. Finer particles (1–2 mm) possess higher specific surface areas than coarser ones (3

mm), promoting rapid surface decomposition and volatile release.[33] Conversely, larger particles exhibit slower decomposition rates, allowing prolonged diffusion of reaction intermediates toward the surface and consequently increasing liquid smoke yield.[34] Particle size also governs mass and heat transfer during pyrolysis.[35] Smaller particles enhance mass transfer due to their larger surface-to-volume ratio[24], while larger particles favour longer heat retention, extending residence time and facilitating more complete pyrolysis reactions.[36] The process generally proceeds through two stages: heating and decomposition.[37]
In larger particles, the formation of less oxidised zones enables more uniform thermal degradation, whereas smaller particles experience faster heating and earlier reaction completion, leading to reduced liquid smoke yields. Thermal conductivity further determines the efficiency of heat transfer within the particles. Particles with higher conductivity distribute heat more effectively, accelerating pyrolysis.[38] In contrast, particles with lower conductivity, such as those of 3 mm size, undergo slower heat transfer, allowing extended reaction time and higher liquid smoke production.[39] At 180°C, 2 mm particles produced the highest yield, attributed to their optimal balance of surface area and internal heat distribution. Meanwhile, 3 mm particles exhibited uneven heat transfer and reduced liquid yield due to slower internal heating and less uniform temperature distribution.

Statistical Analysis Model Fitting
RSM response used the FCCD method using the Design Expert version 13 program. The results of the experiment used RSM with a yield response of 20 experimental units. In this optimisation result, the free variable A was temperature (℃), B was size (mm), and C was time (min) with 1 response, namely liquid smoke yield. The experimental yield varied between 6.51% and 30.43%. ANOVA analysis (Table-3) revealed that the chosen 2FI model was statistically significant ($p < 0.0001$), demonstrating that temperature, particle size, and time all significantly influenced the yield.

Table-3: ANOVA of Linear Response Models Identified Key Factors Influencing Liquid Smoke Yield

Source	Sum of Squares	df	Mean Square	F-value	p-value	
Model	795.09	6	132.51	82.03	<0.0001	significant
A-temperature	110.97	1	110.97	68.70	<0.0001	
B-size	147.83	1	147.83	91.51	<0.0001	
C-time	485.07	1	485.07	300.27	<0.0001	
AB	44.32	1	44.32	27.44	0.0002	
AC	0.5768	1	0.5768	0.3571	0.5604	
BC	6.32	1	6.32	3.91	0.0695	
Residual	21.00	13	1.62			
Lack of Fit	18.53	8	2.32	4.70	0.0526	Not significant
Pure Error	2.47	5	0.4933			
Cor Total	3816.09	19				

As shown in Table-3, the model was highly significant ($F = 82.03$) with only a 0.01% chance of error due to noise. The p-value (<0.05) confirmed that temperature (A), particle size (B), time (C), and their interaction (AB) significantly affected the yield response, while terms with $p > 0.1$ were insignificant. The Lack of Fit test ($F = 4.70$, $p = 0.0526$) indicated a moderate model inaccuracy, though still acceptable within the 5% error margin. As presented in Table-4, the model exhibited strong predictive accuracy with $R^2 = 0.9624$ and Adjusted $R^2 = 0.9128$ (difference < 0.2). The high R^2 value indicated that most of the variation in yield was explained by the model variables. The Adeq Precision ratio of 30.361 (>4) further confirmed a sufficient signal-to-noise ratio, validating the model's reliability for process optimisation.

Tabel-4: Model Analysis for Response

Model	R^2	Adjusted R^2	Predicted R^2	Adeq Precision
2Fl model	0.9743	0.9624	0.9128	30.3614

Optimisation of Coconut Shell Liquid Smoke
Response surface analysis identified the ideal MAP parameters for producing coconut shell liquid. The interaction between temperature, particle size, and time on yield percentage is illustrated in Fig.-4 and expressed through the linear regression model in Eq.-3.

$$Y = 17.13 + 3.72\ A + 4.30\ B + 6.96\ C + 3.33\ AB + 0.3797\ AC + 1.26\ BC \quad (3)$$

The contour and response surface plots (Fig.-4) illustrate the relationship between yield percentage and the independent variables are temperature, particle size, and heating time.[40] An optimal point located near the plot centre indicates that the model accurately represents the variable–response relationship for liquid smoke production using the MAP method with activated charcoal as an absorbent.

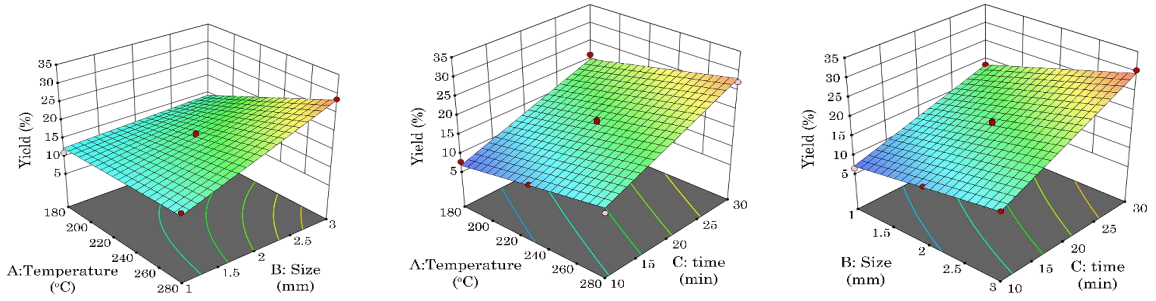

Fig.-4: The Influence of Temperature and Size (a), Temperature and Time (b), and Size and Time (c) on the Production of Liquid Smoke is Displayed on the Response Surface

The effect of temperature and particle size on liquid smoke output is shown in Fig.-4(a). The correspondence between actual (red/white) data points and the predicted surface confirms the model's accuracy. The colour gradient and contour indicate the optimum yield at higher temperatures (280°C) and medium particle size (2 mm). Figure-4(b) shows the interaction between temperature and time, where the nearly flat surface suggests a linear relationship. Yield increases consistently with higher temperature and longer heating time, indicating weak interaction between these variables. Figure-4(c) presents the interaction between particle size and time. The linear and sloping surface implies that both factors independently influence yield with minimal interaction effects.

Table-5: Optimal Values of Variables and Responses

Temperature	Size	Time	Yield	Desirability	
254,950	2,841	28,693	31,133	1,000	Selected

Optimal yield (31.13%) was obtained under conditions of 255°C, 28.7 minutes heating time, and 2.8 mm particle size. The desirability value of 1.000 indicated a 100% model accuracy, confirming the reliability of these parameters as the optimal conditions. As shown in Fig.-5(a), the contour plot of temperature versus size displayed a desirability of 1.000 (red region) at a time of 28.69 min, indicating high model precision. Similarly, Fig.-5(b) illustrates the temperature–time contour, showing a desirability of 1.000 at a particle size of 2.84 mm, further validating the optimization results. Figure-5(c) presents the contour plot of size versus time, showing an optimum desirability value of 1.000 at an actual temperature of 254.95°C.

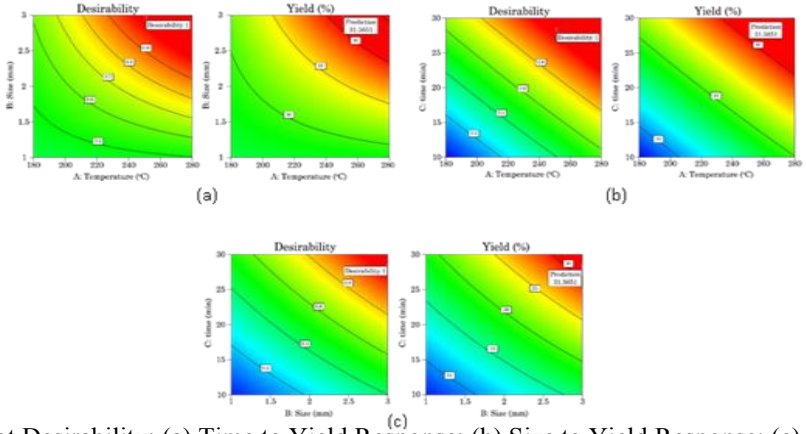

Fig.-5: Contour Plot Desirability: (a) Time to Yield Response; (b) Size to Yield Response; (c) Temperature to Yield Response

Figure-6 shows the relationship between expected and actual liquid smoke yields. The data closely follow a linear trend, indicating strong agreement between experimental results and the predictions from Design Expert 13.

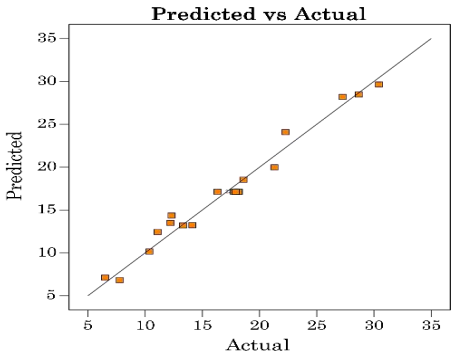

Fig.-6: Distribution of Actual Values and Predicted Values

The predictive versus actual value plot demonstrated high model accuracy and good experimental precision, as data points closely followed the linear trend, indicating strong agreement between predicted and observed results.

CONCLUSION

In the MAP process, activated charcoal was the most effective absorbent, achieving 114.67% effectiveness at a 3 mm particle size, superior to biochar and regular charcoal. Liquid smoke yield varied with temperature and particle size: 23.99% at 180°C (2 mm), 30.43% at 230°C, and 34.40% at 280°C (both 3 mm). The optimal yield of 31.13% occurred at 255°C, 2.8 mm, and 28.7 min. MAP using activated charcoal and 3 mm particles proved efficient for producing high-quality coconut shell liquid smoke, offering promising potential for food industry applications.

ACKNOWLEDGMENTS

I would like to thank the Kemendiktisaintek for the provision of Regular Fundamental research grants and Tribhuwana Tunggadewi University for their support in conducting this research.

CONFLICT OF INTERESTS

The authors declare that there is no conflict of interest.

AUTHOR CONTRIBUTIONS

The present work is related to *Goal-7: Affordable and Clean Energy*. All the authors contributed significantly to this manuscript, participated in reviewing/editing and approved the final draft for publication. The research profile of the authors can be verified from their ORCID ids, given below:

S.P.A. Anggraini https://orcid.org/0000-0002-1710-0417
A.C.K. Fitri https://orcid.org/0000-0002-5646-0722
F.K. Widyastuti https://orcid.org/0009-0003-9606-0517
B. Prihatiningsih https://orcid.org/0000-0002-6809-0693
M. Mahfud https://orcid.org/0000-0001-7740-9670
M.F. Rizki https://orcid.org/0009-0000-4322-626X
T. Sari https://orcid.org/0009-0006-0318-8223
B. Sardi http://orcid.org/0000-0001-9555-0301
N. Indayaningsih https://orcid.org/0000-0003-2148-8976
A. Hapid https://orcid.org/0000-0001-9697-3699
N.I.F. Nisa https://orcid.org/0000-0001-8117-1802
A. Aminudin https://orcid.org/0000-0002-9069-9032
J. Surif https://orcid.org/0000-0001-8383-6601

Cite this article as: S.P.A. Anggraini *et al.*, *Rasayan J. Chem.*, 19(1), 207-216(2026), https://doi.org/10.31788/RJC.2026.1919599.

REFERENCES

1. A.R. Putri, K. Awidarta, B.R.P. Ihsan, I. Khaerunisa, M.B. Ulum and L.F. Huda, *Journal of Food and Pharmaceutical Sciences*, **12**, 28 (2024), https://doi.org/10.22146/jfps.10060
2. M. Sehol, K. Kasmawati, N. Narsito, S.J. Santosa, J. Jumina, R. Sholehah, Z.D. Firdaus, M. Mahfud, M.A. Ardiputra and B. Sardi, *Rasayan Journal of Chemistry*, **18(4)**, 2012(2025), http://doi.org/10.31788/RJC.2025.1849396
3. R. Ruslan, B. Sardi, K. Khairuddin, N.K. Sumarni, W. Tiro, Z. P. Magfira, N. Ainun and M. Mahfud, *Journal of the Energy Institute*, **119**, 101942(2025), https://doi.org/10.1016/j.joei.2024.101942
4. D. Mansur, S. Sugiwati, W.A. Rizal, R. Suryani and R. Maryana, *Biomass Conversion and Biorefinery*, **13**, 10561 (2023), https://doi.org/10.1007/s13399-021-01896-x
5. B. Sardi, R.F. Ningrum, V.A. Ardiansyah, L. Qadariyah and M. Mahfud, *International Journal of Technology*, **13**, 147(2022), https://doi.org/10.14716/ijtech.v13i1.4358
6. X. Xin, K. Dell, I.A. Udugama, B.R. Young and S. Baroutian, *Journal of Cleaner Production*, **294**, 125368 (2021), https://doi.org/10.1016/j.jclepro.2020.125368
7. W. A. Rizal, K. Nisa', R. Maryana, D. J. Prasetyo, D. Pratiwi, T. H. Jatmiko, D. Ariani and A. Suwanto, *IOP Conference Series: Earth and Environmental Science*, **462**, 012057(2020), https://doi.org/10.1088/1755-1315/462/1/012057
8. C. Qiang, W. Yan and Z. Huamin, *Chemistry and Industry of Forest Products*, **40**, 45(2020), https://doi.org/10.3969/j.issn.0253-2417.2020.01.007
9. S. Maulina, R. Amalia and E. R. Kamny, *E3S Web of Conferences*, **148**, 02007(2020), https://doi.org/10.1051/e3sconf/202014802007
10. H. A. Oramahi, K. Kustiati and E. R. P. Wardoyo, *Science and Technology Indonesia*, **7**, 257(2022), https://doi.org/10.26554/sti.2022.7.2.257-262
11. M. Masfria, H. Syahputra, H. S. Wahyuni, N. F. Zebua, E. Elizabeth and M. Marcelynn, *Pharmacy Education*, **24**, 39(2024), https://doi.org/10.46542/pe.2024.242.3945
12. M. Mahfud, A.H. Ramadhana, N.A. Novita, F. Kurniawansyah, B. Sardi, M. Mirzan, L. Mahmudin, A.A. Ali and N. Indrawan, *Energy*, **341**, 134309(2025), https://doi.org/10.1016/j.energy.2024.134309
13. B. Sardi, I. Uno, F.A. Marhum, A.A. Akbar, T. Arief, M. Arif, A. Altway and M. Mahfud, *International Journal of Hydrogen Energy*, **49**, 203(2024), https://doi.org/10.1016/j.ijhydene.2023.07.217
14. T.K. Dhaniswara, B. Sardi, S.R. Juliastuti and M. Mahfud, *Cleaner Waste Systems*, **11**, 100305(2025), https://doi.org/10.1016/j.clwas.2025.100305
15. M. Sehol, K. Kasmawati, N. Narsito, S.J. Santosa, J. Jumina, R. Sholehah, Z.D. Firdaus, M. Mahfud, M.A. Ardiputra and B. Sardi, *Rasayan Journal of Chemistry*, **18(4)**, 4(2025), https://doi.org/10.31788/RJC.2025.1849396
16. Q. Fan, C. Song and P. Fu, *Journal of Cleaner Production*, **434**, 140118(2024), https://doi.org/10.1016/j.jclepro.2023.140118
17. N. Nurhaeni, E.A. Rahim, A.A. Amar, M.A. Ardiputra and B. Sardi, *Rasayan Journal of Chemistry*, **18(2)**, 1004(2025), https://doi.org/10.31788/RJC.2025.1829293
18. S. P. A. Anggraini, S. Suprapto, S. R. Juliastuti and M. Mahfud, *International Journal of Renewable Energy Development*, **13**, 145 (2024), https://doi.org/10.14710/ijred.2024.56287
19. F. C. Dewi, S. Tuhuteru, A. Aladin and S. Yani, *Journal of Environmental and Agricultural Studies*, **2(2)**, 81(2021), https://doi.org/10.32996/jeas.2021.2.2.7
20. K. Khairuddin, M.A. Ridhawansa, R. Ruslan and B. Sardi, *Cleaner Waste Systems*, **10**, 100225(2025), https://doi.org/10.1016/j.clwas.2025.100225

21. B. Sardi, H. Rachmawati, T. Fakhry, E. Setiawati, N. Indrawan, M. Mahfud, *Bioresource Technology Reports*, **21**, 101367(2023), https://doi.org/10.1016/j.biteb.2023.101367
22. Y. Zheng, T. Zheng, A. Li, Y. Huang, M. Usman, C. Liao, Q. Deng and H. Yao, *Journal of Cleaner Production*, **511**, 145631 (2025), https://doi.org/10.1016/j.jclepro.2025.145631
23. M.I. Taipabu, B.Y. Chou, W. Wu, B. Sardi, *Applied Thermal Engineering*, **278**, 127457(2025), https://doi.org/10.1016/j.applthermaleng.2025.127457
24. K. Ridhuan, D. Irawan and R. Setiawan, *Journal of Engineering and Scientific Research*, **2**, 10 (2020), https://doi.org/10.23960/jesr.v2i1.37
25. M. Mahfud, R. Rachmaditasari, A. Ansori, A. Suryanto, B. Sardi, *Biocatalysis and Agricultural Biotechnology*, **67**, 103657(2025), https://doi.org/10.1016/j.bcab.2025.103657
26. T. Zhu, Y. Sun, Y. Wang, H. Xing, X. Li, P. Hu, Y. Zong and X. Zheng, *Journal of Materials Science: Materials in Electronics*, **31**, 6843 (2020), https://doi.org/10.1007/s10854-020-03244-7
27. Q. Fan, C. Song, Y. Sun, D. Wang, E. Bennett, J. Xiao and P. Fu, *Journal of Cleaner Production*, **507**, 145538 (2025), https://doi.org/10.1016/j.jclepro.2025.145538
28. Y. X. Gan, *Journal of Carbon Research*, **7**, 39 (2021), https://doi.org/10.3390/c7020039
29. W. Gu, J. Shi, J. Zhang, Q. Jia, C. Liu, H. Ge, Q. Sun and L. Zhu, *Molecules*, **28**, 6419(2023), https://doi.org/10.3390/molecules28176419
30. A. S. L. Pérez, J. J. L. Castro and C. A. G. Fajardo, *Journal of Manufacturing and Materials Processing*, **8**, 121 (2024), https://doi.org/10.3390/jmmp8030121
31. S. Y. Foong, R. K. Liew, P. N. Y. Yek, C. S. Han, X. Y. Phang, X. Chen, W. W. F. Chong, M. Verma and S. S. Lam, *Energy*, **272**, 127178 (2023), https://doi.org/10.1016/j.energy.2023.127178
32. S. Y. Foong, Y. H. Chan, S. S. M. Lock, B. L. F. Chin, C. L. Yiin, K. W. Cheah, A. C. M. Loy, P. N. Y. Yek, W. W. F. Chong and S. S. Lam, *Bioresource Technology*, **369**, 128478(2022), https://doi.org/10.1016/j.biortech.2022.128478
33. K. S. Ukanwa, K. Patchigolla, R. Sakrabani, E. Anthony and S. Mandavgane, *Sustainability*, **11**, 6204 (2019), https://doi.org/10.3390/su11226204
34. C. Cheng, Q. Guo, L. Ding, Y. Gong and G. Yu, *Journal of Cleaner Production*, **448**, 141701 (2024), https://doi.org/10.1016/j.jclepro.2024.141701
35. E.A. Rahim, M.I. Al Bafadhal, W. Azizah, R.A.P. Prastyo, N.K. Sumarni and B. Sardi, *Journal of The Tuskish Chemical Society A*, **11**, 925(2024), https://doi.org/10.18596/jotcsa.136723
36. F. Y. Han, M. Wang, X. B. Ma, L. J. Yin, D. Z. Chen, Z. Q. Liu and R. N. Zhang, *Heliyon*, **9**, e21255 (2023), https://doi.org/10.1016/j.heliyon.2023.e21255
37. S. Mariyam, T. A. Ansari and G. McKay, *Energy Sources, Part A: Recovery, Utilisation, and Environmental Effects*, **45**, 3681 (2023), https://doi.org/10.1080/15567036.2023.2196945
38. B. Sardi, I. Uno, F. Pasila, A. Altway and M. Mahfud, *FirePhysChem*, **3**, 106(2023), https://doi.org/10.1016/j.fpc.2023.02.002
39. S. A. Novita, S. Santosa, N. Nofialdi, A. Andasuryani, A. Fudholi, A. Azril, R. Zainul, *Journal of Medicinal and Pharmaceutical Chemistry Research*, **6**, 12677(2024), https://doi.org/10.3390/app122412677
40. B. Sardi, A. Altway and M. Mahfud, *Fuel*, **324**, 124509(2022), https://doi.org/10.1016/j.fuel.2022.124509

[RJC-9599/2025]